Applied Physics Letters

RESEARCH ARTICLE | MARCH 23 2026

Counter-rotating electromagnetic generator with planetary gear amplification for low-frequency wave energy harvesting

FREE

Chengyun Du; Xiaoning Wang ; Yizhou Li ; Yawei Wang ; Lihua Tang ; Yupei Jian ; Quanke Su; Guobiao Hu

Appl. Phys. Lett. 128, 123901 (2026)
https://doi.org/10.1063/5.0316349

AIP Publishing

Applied Physics Letters ARTICLE pubs.aip.org/aip/apl

Counter-rotating electromagnetic generator with planetary gear amplification for low-frequency wave energy harvesting

Cite as: Appl. Phys. Lett. **128**, 123901 (2026); doi: 10.1063/5.0316349
Submitted: 12 December 2025 · Accepted: 9 March 2026 ·
Published Online: 23 March 2026

View Online Export Citation CrossMark

Chengyun Du,[1] Xiaoning Wang,[2] Yizhou Li,[1] Yawei Wang,[1] Lihua Tang,[2] Yupei Jian,[3,a)] Quanke Su,[4] and Guobiao Hu[1,a)]

AFFILIATIONS

[1]Thrust of Internet of Things, The Hong Kong University of Science and Technology (Guangzhou), Guangzhou, Guangdong 511400, China
[2]Department of Mechanical and Mechatronics Engineering, The University of Auckland, Auckland 1010, New Zealand
[3]School of Electrical Engineering, Southwest Jiaotong University, Chengdu 610031, China
[4]Thrust of Intelligent Transportation, The Hong Kong University of Science and Technology (Guangzhou), Nansha, Guangzhou 511400, China

[a)]**Authors to whom correspondence should be addressed:** yupeijian@swjtu.edu.cn and guobiaohu@hkust-gz.edu.cn

ABSTRACT

Ocean wave energy represents a promising renewable resource with high energy density. However, its inherently low-frequency, stochastic, and multi-directional characteristics pose significant challenges for efficient energy harvesting. In this study, a pendulum-type counter-rotating electromagnetic generator (CREMG) is proposed to address these issues. The CREMG integrates a planetary gear system and dual one-way bearings. The one-way bearings convert irregular bidirectional pendulum motion into unidirectional rotation, and the planetary gear system amplifies the rotation by a 1:4 transmission ratio, collectively enhancing energy conversion efficiency. Experimental results show that the proposed CREMG delivers a maximum RMS power of 304.46 mW at an optimal load resistance of 5000 Ω, with a 1 F capacitor charged to 3.44 V within 400 s, corresponding to a harvested energy of 5.92 J. To further validate its practical potential, the CREMG was used to power a customized wireless sensing circuit for temperature and humidity monitoring under random excitations. Overall, this work demonstrates a compact and efficient solution for low-frequency wave energy harvesting, offering a viable pathway toward self-powered marine sensing and autonomous ocean monitoring systems.

Ocean waves, one of the most abundant renewable energy resources on Earth, have garnered increasing attention in recent years.[1,2] However, converting wave motions into electrical energy remains challenging due to the inherent randomness, low frequency, and multi-directional nature of ocean waves.[3–5] To address these challenges, researchers have proposed a wide range of wave energy harvesting systems that leverage innovative structural architectures[6,7] and various energy transduction mechanisms.[8–10]

From the perspective of structural design, numerous structural innovations have been proposed to enhance energy harvesting efficiency and better accommodate the low-frequency characteristics of ocean waves.[11–13] Tang *et al.*[14] employed a Mag-Boost mechanism that could convert ultra-low-frequency excitations below 1 Hz into high-frequency oscillations exceeding 50 Hz in the power magnet without direct mechanical contact. This design significantly improved the energy harvester's output performance, achieving a maximum power of 1.79 W and a power density of 1.88 kW/m^3. Cai and Zhu[15] designed a double-mass pendulum (DMP) oscillator whose natural frequency could be tuned by adjusting the positions of two independent masses. The proposed system exhibits tunable natural frequencies ranging from 0.2 to 1.4 Hz, and it delivers an average output power of 100 mW when subjected to a wave period of 0.7 s and a wave height of 0.1 m.

From the aspect of energy conversion, three primary transduction mechanisms are commonly employed: piezoelectric,[16–18] triboelectric,[3,19,20] and electromagnetic.[21,22] Among them, piezoelectric harvesters are capable of producing relatively high voltages under low-frequency excitations,[18] but their power output is constrained by

inherently high internal resistances.[23] Triboelectric harvesters offer lightweight structures, ease of fabrication, and high voltage outputs; however, their power densities remain relatively low. Moreover, surface charge dissipation reduces their long-term durability, especially in humid marine environments.[3,24] Electromagnetic harvesters can deliver larger current and higher overall power density, but they typically require sufficient relative motion between magnets and coils to achieve effective energy conversion,[25,26] making them less efficient under small-amplitude and low-frequency excitations. To overcome the inherent limitations of individual mechanisms, hybrid energy harvesters that synergize multiple transduction mechanisms have been widely explored as a potential solution.[27–29] For instance, He *et al.*[30] proposed a piezoelectric-electromagnetic hybrid energy harvester (PEHEH) that couples the high-voltage sensitivity of piezoelectric materials with the high current output of electromagnetic induction. Their device integrates L-shaped piezoelectric cantilevers with multiple electromagnetic generators, allowing large deformation at low frequencies while enhancing magnetic flux variation through moving spherical magnets. The hybrid harvester achieved a maximum output power of 32.58 mW, sufficient to power multiple LEDs, demonstrating improved adaptability under low-frequency marine excitations. However, despite the enhanced performance of hybrid configurations, their increased structural complexity, higher cost, and reduced reliability pose challenges for long-term deployment in marine environments.

To achieve a compact yet efficient solution for irregular, low-frequency, multi-directional wave excitations, this study proposes a counter-rotating electromagnetic generator (CREMG) equipped with a planetary gear mechanism for amplifying input motion. Furthermore, the proposed design transforms irregular bidirectional excitations into continuous unidirectional rotation through one-way bearings, thereby enhancing the conversion efficiency. A comprehensive experimental evaluation was conducted to characterize its power generation performance. The prototype achieved remarkable output capability and powered a wireless sensing node for temperature and humidity monitoring, highlighting its strong potential for practical applications.

As shown in Fig. 1(a), the proposed CREMG is designed to be embedded within an ocean buoy [Fig. 1(b)], where the pendulum is driven by the buoy's motion induced by ocean wave excitations. The resulting relative rotation of the pendulum provides the mechanical input, which is then converted into electrical energy through the internal transmission and transduction components.

As shown in Fig. 1(c), the CREMG mainly consists of three functional subsystems: a motion amplification module, a one-way bearing assembly, and a wireless sensing unit. The motion amplification module utilizes a planetary gear system with a 1:4 transmission ratio to enhance the input motion. Inspired by self-winding wristwatch mechanisms,[31,32] this design can transform small, irregular excitations into smooth, continuous rotation for efficient energy conversion.

During operation, as shown in Fig. 1(d), external wave excitation first induces bidirectional swinging of the pendulum, which drives the planetary gear transmission system. Through the coordinated interaction of the sun gear, planet gears, and ring gear, the mechanical input is redistributed within the gear train. The sun gear then drives two one-way bearings that rotate in opposite directions, with the permanent magnets and coils mounted on two separate bearings. Owing to the rectification effect of one-way bearings, the alternating rotational input generated by irregular wave-induced motion is converted into effectively unidirectional rotation at the output stage. Meanwhile, the planetary gear mechanism amplifies the rotational speed, thereby enhancing the relative motion between the magnets and coils. This counter-rotating design not only enhances electromagnetic induction by increasing the relative angular velocity but also ensures more stable, continuous power generation, delivering reliable electromagnetic power to the downstream wireless sensing unit.

The structural details of the proposed CREMG are illustrated in Fig. 2(a), and the key design parameters are listed in Table I. The one-way bearing operates via a ratchet mechanism: when the cover rotates clockwise, the ceramic balls disengage to allow free motion, whereas a reversal of rotation causes the balls to wedge into the locking grooves, halting the backward rotation. This unidirectional locking mechanism ensures that the magnets and coils can rotate consistently in opposite directions, each maintaining a fixed rotational sense despite the bidirectional nature of the input excitation. It is worth noting that, to prevent coil entanglement during rotation, the eight coils are connected in series, with their terminals wound around two bolts. The leads from these bolts are connected to a headphone plug, serving as an electrical interface to deliver the induced voltage, ensuring reliable and stable energy output.

When the pendulum rotates, the system's kinetic energy can be expressed as

$$T=\frac{1}{2}\left\{I_1\left[\left(\frac{N_3}{N_1}+1\right)\dot{\theta}_r\right]^2+I_2\left[\dot{\theta}_a-\left(\frac{N_3}{N_2}+1\right)\dot{\theta}_r\right]^2+\sum_{j=1}^{3}m_j\|v_j\|^2\right\}, \tag{1}$$

where I_1 and I_2 are the moments of inertia of the sun gear and planet gear about their respective center of mass. N_1, N_2, and N_3 represent the tooth numbers of the sun gear, planet gear, and ring gear, respectively. θ_r and θ_a denote the rotational angles of the pendulum with respect to the initial and current vertical axis, respectively. m_j and v_j correspond to the mass and translational velocity of each component (sun gear, planet gear, and pendulum). Equation (1) provides a qualitative mechanical interpretation of the motion amplification mechanism in the CREMG. It offers physical insights into the kinetic energy distribution and gear-induced speed amplification within the pendulum-planetary transmission system, while neglecting electromagnetic damping and circuit coupling; therefore, it is not intended for quantitative evaluation of electrical outputs. During operation, the sun gear drives the magnets and coils to rotate. As the magnets reach different angular positions, the distribution of the magnetic flux density varies accordingly, as illustrated in Fig. 2(b).

A prototype of the CREMG, as shown in Fig. 2(c), was fabricated using a high-precision 3D printer (Bambu X1 Carbon). All components were printed with PLA to ensure geometric accuracy and structural integrity. To achieve precise alignment and reliable mechanical coupling during operation, interlocking features, such as slot-and-pin structures, were incorporated into the design between adjacent components. These modular interconnections enable accurate positioning, reduce assembly tolerance errors, and maintain coaxial alignment of rotating parts. During assembly, the planetary gear set, pendulum, shafts, one-way bearings, magnets, and coils were installed according to the configuration illustrated in Fig. 2(a). The rotating components were mounted onto shafts supported by one-way bearings to ensure smooth motion and reduce mechanical friction. To further enhance

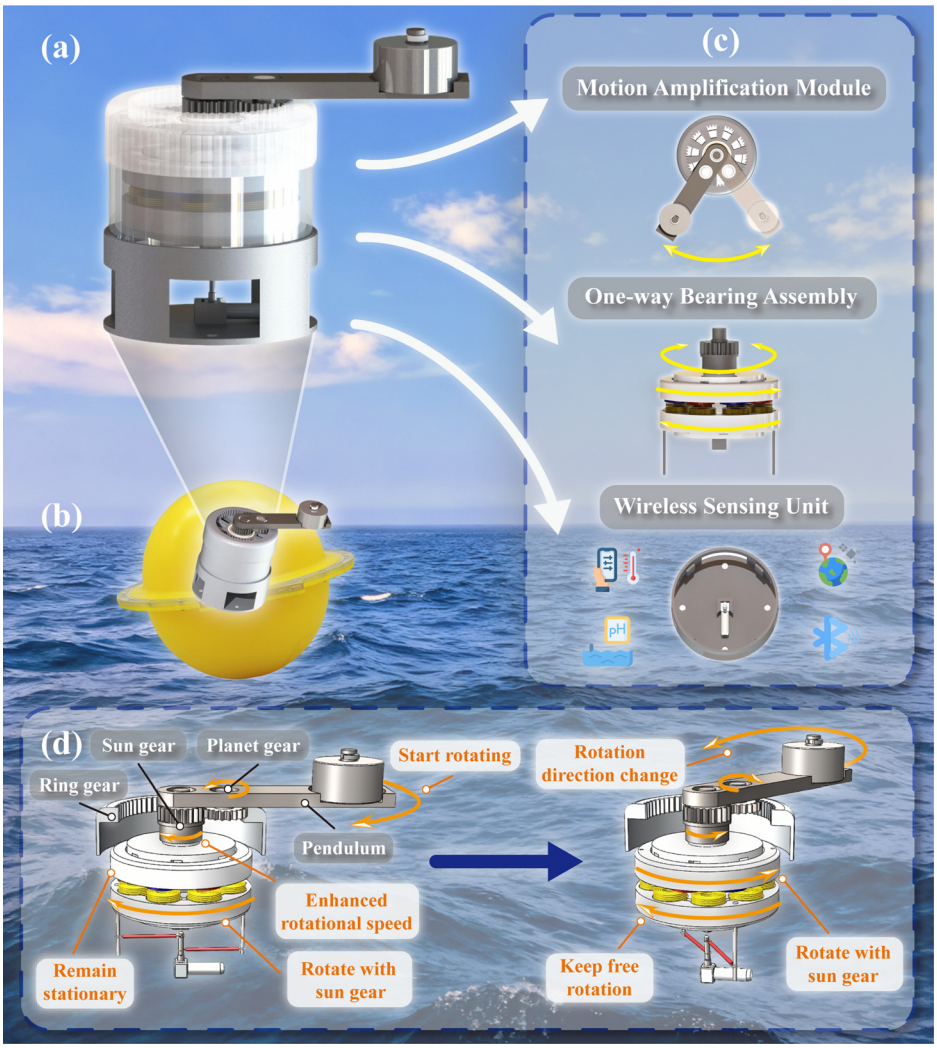

FIG. 1. Structural design (a) and application scenario (b) of the proposed counter-rotating electromagnetic generator (CREMG). (c) Functional subsystems of the CREMG, including the planetary gear module that amplifies input motion, the one-way bearing assembly that rectifies bidirectional excitation into continuous unidirectional rotation, and the wireless sensing unit for autonomous monitoring. (d) Schematic illustration of the transmission mechanism, showing the pendulum-driven planetary gear system and one-way bearings that enable speed amplification and directional rectification under bidirectional excitation.

structural stability under continuous rotation and external excitation, double-sided adhesive tapes were selectively applied at interfaces prone to loosening or vibration-induced separation.

As shown in Figs. 2(d) and 2(e), the experimental setup was rigidly mounted onto the linear motor and the six-degree-of-freedom (6-DOF) platform using customized fixtures and bolted mechanical connections. A dedicated mounting base was designed to match the bottom geometry of the CREMG housing. The bolted fixation and rigid interface effectively prevented undesired vibration, misalignment, or slippage during high-acceleration reciprocating motion and multidirectional excitation, thus ensuring stable and repeatable testing conditions. During the experiments, the output voltage of the CREMG was monitored and recorded using an oscilloscope (RIGOL DHO 1104).

To first validate the effectiveness of the motion amplification and counter-rotating mechanisms, the open circuit voltages of four different configurations are compared in Fig. 3(a). Configuration ⟨i⟩ in Fig. 3(a) serves as the baseline case, in which only the magnets rotate via a single one-way bearing, while the coils remain stationary. In this configuration, the relative angular velocity between the magnets and coils is limited, resulting in a relatively low rate of magnetic flux variation and a small peak open-circuit voltage of 34.69 V. When only the counter-rotating design is introduced [see inset ⟨ii⟩ in Fig. 3(a)], the magnets and coils rotate in opposite directions. This counter-rotation significantly increases the relative angular velocity between the magnets and coils. According to Faraday's law, the induced voltage is proportional to the rate of magnetic flux change; thereby, the enhanced relative motion directly leads to a higher induced voltage of 57.34 V. When the planetary gear system is incorporated without the counter-rotation mechanism, the peak voltage further rises to 66.61 V [see inset ⟨iii⟩ in Fig. 3(a)]. The planetary gear system amplifies the input motion and increases the rotational speed of the sun gear. Finally, when both the planetary gear system and two one-way bearings are simultaneously implemented [see inset ⟨iv⟩ in Fig. 3(a)], the peak open-circuit voltage rises to 113.19 V, which is 3.26 times higher than the baseline, 1.92 times higher than using the planetary gear transmission system alone, and 1.65 times higher than employing only the counter-rotating design. These quantitative results confirm that motion amplification

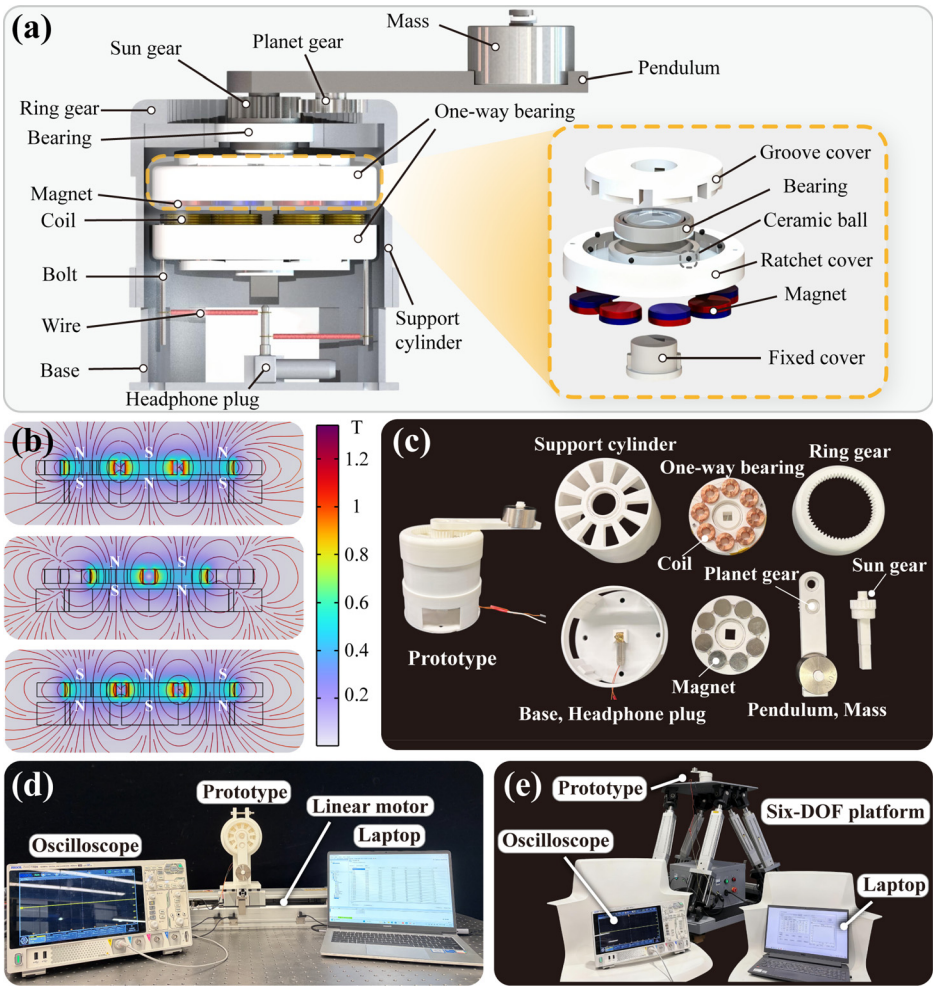

FIG. 2. (a) Sectional drawing of the CREMG showing its internal structure. (b) Simulated magnetic field distribution of the magnet array during rotation. (c) The fabricated prototype and its core components. (d) and (e) The experiment setup for performance evaluation.

TABLE I. Design parameters of the CREMG.

Parameter	Value
Tooth number of sun gear	20
Tooth number of planet gear	20
Tooth number of ring gear	60
Support cylinder	ϕ 96 × 70 mm^2
Pendulum length	126 mm
Mass	50/100/150/200 g
Number of magnets	8
Number of coils	8
Magnet type	N52
Turns of each coil	1350
Wire diameter of the coil	0.15 mm
Resistance of each coil	48 Ω
Bolt specification	M2
Headphone plug type	AVSSZ
Ceramic ball diameter	ϕ 2.778 mm

(via gear ratio-induced speed upconversion) and counter-rotation (via increased relative velocity) act in a complementary manner, substantially boosting the relative motion between magnets and coils and, consequently, the electrical output of the harvester.

To identify the optimal operating condition of the CREMG, its performance was evaluated under varying excitation parameters. Figure 3(b) shows the open-circuit voltage waveforms at different excitation frequencies, with a fixed reciprocating displacement of 180 mm applied by the linear motor. At a low frequency of 0.4 Hz, the output voltage amplitude is small, and the waveform is irregular, indicating that the excitation is insufficient to sustain the stable rotational motion of the internal components. As the excitation frequency increases, the pendulum receives stronger dynamic input per unit time, leading to higher angular velocity after transmission via the planetary gear system. Consequently, the relative rotational speed between the magnets and coils increases, producing a larger rate of magnetic flux variation. The voltage amplitude, therefore, increases, and the waveform becomes smoother and more sinusoidal, reflecting a more stable rotational operation of the generator.

Figure 3(c) demonstrates the variations of peak and RMS voltages with respect to the excitation frequency, showing a maximum output

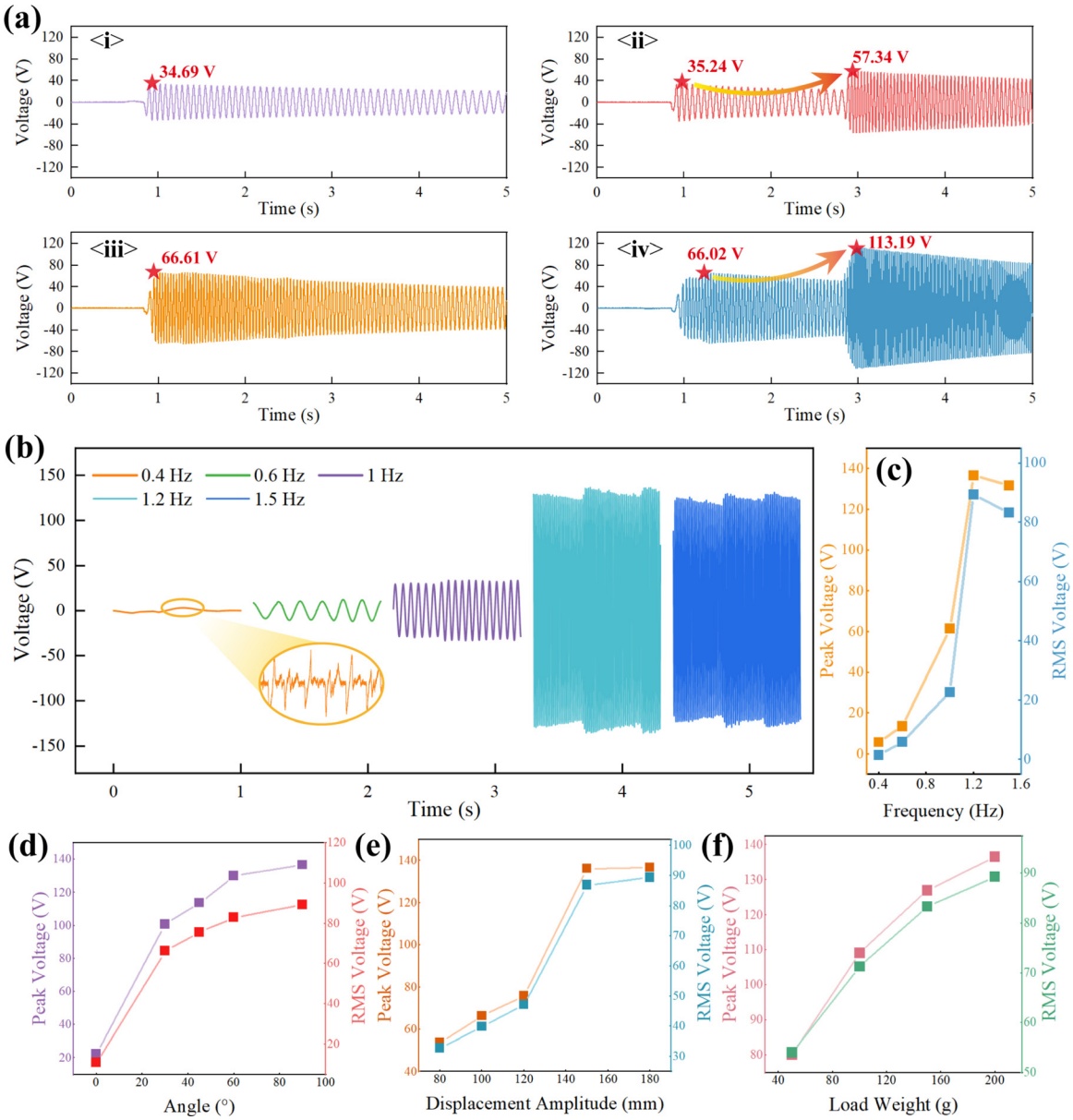

FIG. 3. (a) Comparison of open-circuit voltage waveforms for four configurations, illustrating the effects of the planetary gear and counter-rotating mechanisms. (b) Voltage waveforms of the CREMG under different frequency excitations. (c) Effect of excitation frequency, (d) effect of pendulum inclination angle, (e) effect of displacement amplitude, and (f) effect of pendulum mass on peak and RMS voltages of the CREMG.

attained at 1.2 Hz with peak and RMS voltages of 136.6 and 89.31 V, respectively. This result can be attributed to dynamic matching between the excitation frequency and the intrinsic response characteristics of the pendulum-gear system. Around 1.2 Hz, the system operates closer to its optimal dynamic condition, enabling enhanced rotational speed and efficient energy transfer. At frequencies lower or higher than this value, the pendulum response amplitude and transmission efficiency decrease, resulting in reduced output.

Figures 3(d)–3(f) further reveal the effects of several key structural and excitation parameters, including the pendulum inclination angle (0°–90°), displacement amplitude (80–180 mm), and pendulum mass (50–200 g). Increasing the inclination angle enhances the effective gravitational torque acting on the pendulum, leading to larger angular motion and higher output voltage. Similarly, larger displacement amplitudes supply greater mechanical input energy from the linear motor, directly increasing pendulum swing amplitude and rotational speed after gear amplification. Increasing the pendulum

mass increases the system's kinetic energy under the same excitation, strengthening the inertial effect and contributing to more pronounced rotational motion. In all three cases, enhanced mechanical motion translates into higher relative angular velocity between magnets and coils, and thus greater electromagnetic output. Considering the combined effects of the above parameters, the optimal operating condition is identified when a 200 g pendulum is positioned vertically (90°) with a displacement amplitude of 180 mm and an excitation frequency of 1.2 Hz. Under this condition, the system achieves the highest voltage output, demonstrating optimal mechanical energy conversion and transmission efficiency.

Figure 4(a) presents the electrical output of the CREMG under optimal excitation conditions. The power increases with the load resistance and peaks at the optimal load of 5000 Ω, corresponding to a maximum RMS power of 304.46 mW. Using this value, the power density was calculated based on the device volume for fair comparison with previous studies. As summarized in Table II, the proposed design achieves a markedly higher power density than other reported devices.[22,33–36] To assess the CREMG from a more application-oriented perspective, capacitor charging tests were conducted, with the results presented in Fig. 4(b). The CREMG charged capacitors of 0.33, 1, 1.5, and 2 F to 4.45, 3.44, 2.48, and 1.58 V in 400 s, respectively. The corresponding collected energies, calculated from the capacitor voltages, are 3.27, 5.92, 4.61, and 2.49 J, as shown in Fig. 4(c). The average charging powers under these conditions are 8.18, 14.81, 11.52, and 6.21 mW, respectively.

In real ocean conditions, wave excitations are random and dynamic, characterized by continuously changing amplitudes, frequencies, and directions. Therefore, a constant and periodic input, as used in controlled experiments, cannot fully represent practical conditions. To emulate realistic sea states, additional tests were performed on a 6-DOF platform. In the test, the CREMG was mounted in both horizontal (0°) and vertical (90°) orientations. Its capacitor charging performance under random excitations was recorded, with the results shown in Figs. 4(d) and 4(e). When mounted horizontally, the CREMG exhibits significantly higher charging performance than when mounted vertically. The capacitor voltages reach 0.63 and 0.844 V in the horizontal orientation, far exceeding those obtained in the vertical

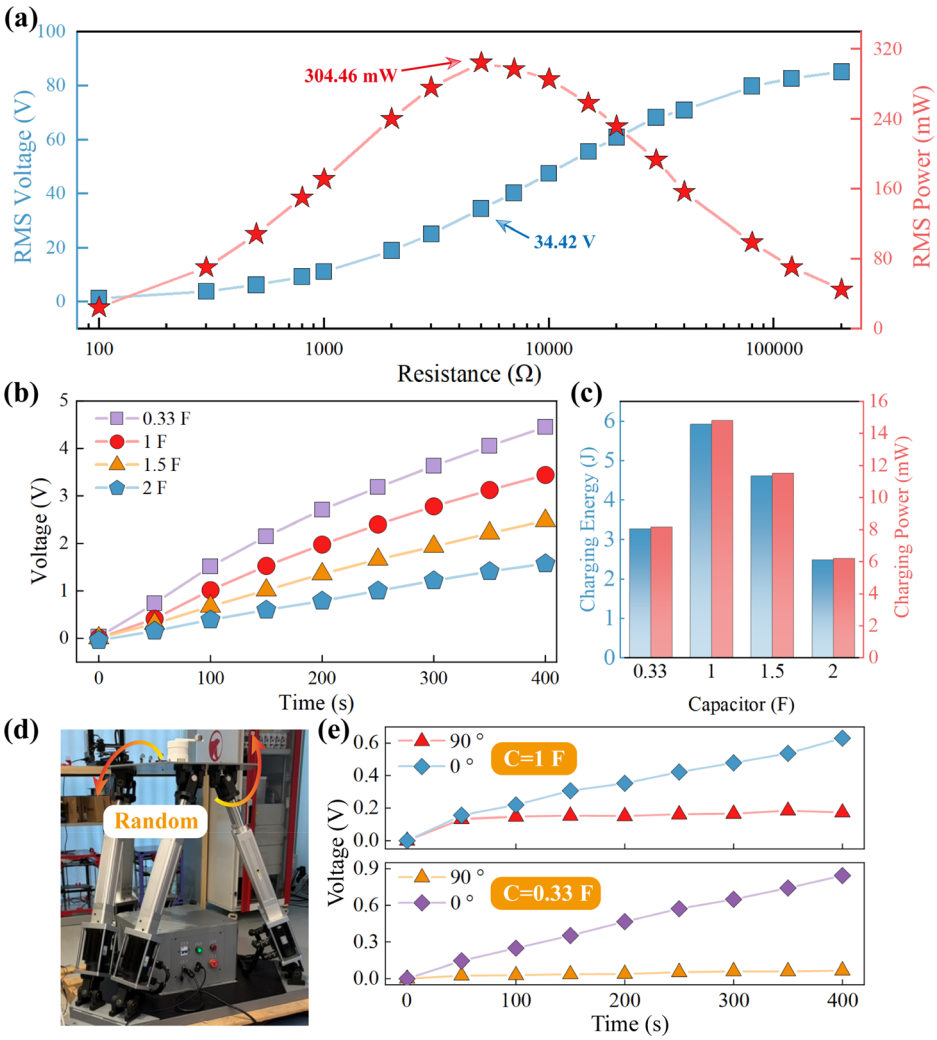

FIG. 4. (a) Outputs of the CREMG under different load resistances. (b) Recorded voltage curves during capacitor charging. (c) Harvested energy and average power for charging different capacitors. (d) Experimental setup on the 6-DOF platform under random excitation. (e) Charging performance of the CREMG in horizontal (0°) and vertical (90°) orientations.

TABLE II. Comparison of this work with other representative studies. EMG = electromagnetic generator; TENG = triboelectric nanogenerator; PEH = piezoelectric energy harvester.

Reference	Type	Volume (cm^3)	RMS power (mW)	Power density (mW/cm^3)
Lou *et al.*[22]	EMG	3 600	920	0.256
Hou *et al.*[33]	EMG	116.64	53.28 (AVE)	0.457
Zhao *et al.*[34]	EMG+TENG	1 773	120	0.046
Jia *et al.*[35]	EMG+PEH	3 000	420	0.14
Wang and Wang[36]	EMG	29 000	295	0.0102
This work	EMG	470.25	304.46	0.647

mode. This demonstrates that, under stochastic excitations, the horizontally oriented CREMG can more effectively harness kinetic energy from multi-directional motions, thereby enhancing its energy harvesting efficiency.

To demonstrate the practical applicability of the proposed CREMG, a self-powered wireless temperature and humidity sensing system was developed, as shown in Fig. 5. The system integrates the CREMG, an energy management circuit, a storage capacitor, and a Bluetooth Low Energy (BLE) module. Under random excitation, the harvested energy is intermittently stored and released to power the sensing unit. As shown in Fig. 5(c), the system performs environmental sensing and reliably transmits the measured data via BLE. The evolution of the capacitor voltage confirms stable energy accumulation and regulated discharge during operation. This application demonstration validates that the proposed CREMG can reliably sustain low-power wireless sensing tasks under irregular excitation conditions.

In this study, a pendulum-type counter-rotating electromagnetic wave energy harvester (CREMG) integrating a planetary gear motion amplification system and dual one-way bearing mechanisms was

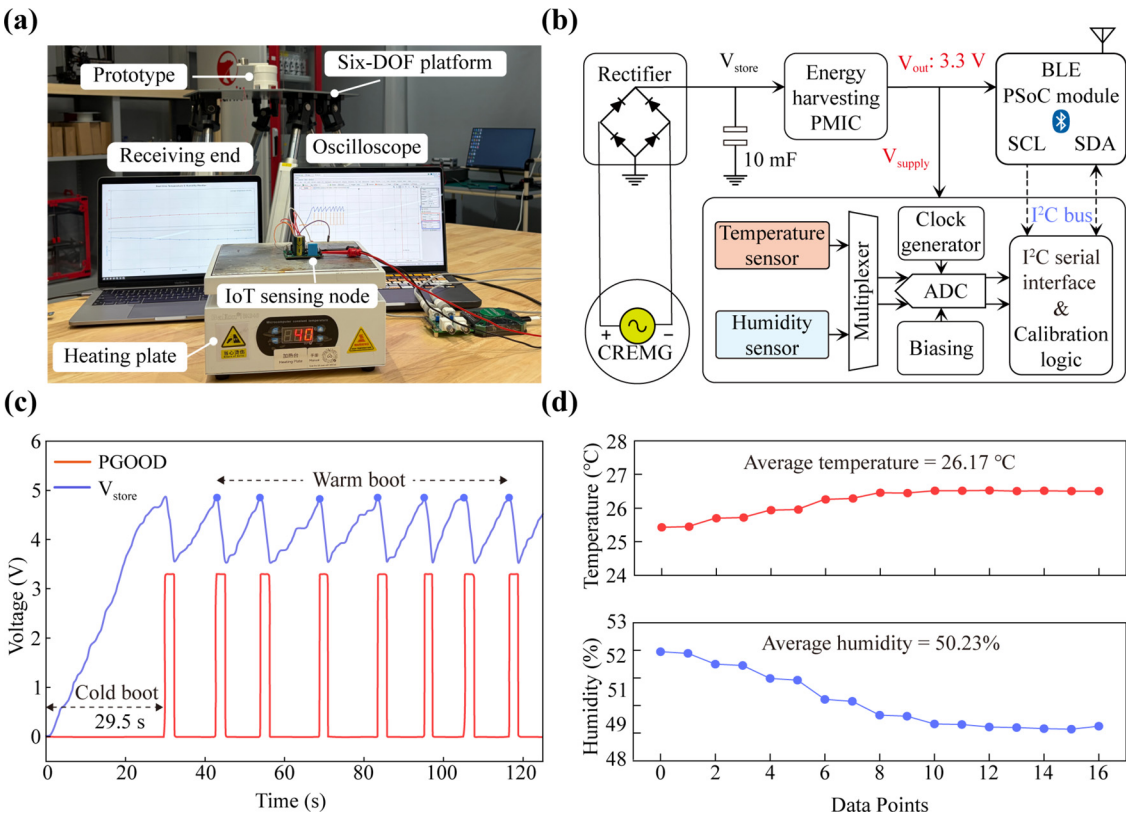

FIG. 5. (a) Physical layout of the experimental setup for showcasing the real-world applicability of the proposed CREMG. (b) Schematic of the self-powered IoT sensing platform. (c) Time-history voltage across the 10 mF capacitor and the PGOOD pin during successive charging and discharging cycles, showing cold-boot and warm-boot operations. (d) Temperature and humidity data received via Bluetooth, confirming environmental sensing powered solely by the CREMG.

proposed and experimentally validated for efficient low-frequency wave energy harvesting. The design enables the conversion of random, bidirectional excitations into continuous unidirectional rotation, significantly improving electromagnetic energy conversion efficiency. Experimental results showed that the CREMG could deliver a maximum RMS power of 304.46 mW under optimal load conditions. Additionally, a 1 F capacitor could be charged to 3.44 V within 400 s, corresponding to a harvested energy of 5.92 J, confirming its strong energy harvesting capability. The practical applicability of the proposed CREMG was showcased through powering a customized wireless sensing unit for temperature and humidity monitoring under random excitations. In summary, the proposed energy harvester paves the way for maintenance-free ocean monitoring systems and contributes to the advancement of autonomous, self-powered maritime technologies.

See the supplementary material for more details of the experimental demonstration of the CREMG-powered wireless sensing system. It also provides a detailed description of the system configuration, energy management, and operating cycles of the self-powered sensing unit, including the cold- and warm-boot behavior, as well as the wireless transmission of temperature and humidity data. These results further demonstrate the feasibility of powering wireless environmental sensing using the proposed harvester under random excitations.

This study was financially supported by the National Natural Science Foundation of China (Grant Nos. 52305135 and 52505130), the Guangdong Provincial Project (Grant No. 2023QN10L545), and the Sichuan Science and Technology Program (Grant No. 2025ZNSFSC1268).

AUTHOR DECLARATIONS

Conflict of Interest

The authors have no conflicts to disclose.

Author Contributions

Chengyun Du and Xiaoning Wang contributed equally to this paper.

Chengyun Du: Data curation (equal); Formal analysis (equal); Investigation (equal); Methodology (equal); Software (equal); Validation (equal); Visualization (equal); Writing – original draft (equal). **Xiaoning Wang:** Data curation (equal); Formal analysis (equal); Investigation (equal); Methodology (equal). **Yizhou Li:** Data curation (equal); Formal analysis (supporting); Investigation (equal); Methodology (supporting); Software (equal); Visualization (supporting). **Yawei Wang:** Formal analysis (supporting); Investigation (supporting); Methodology (supporting); Software (supporting). **Lihua Tang:** Methodology (equal); Project administration (supporting); Supervision (supporting); Writing – review & editing (supporting). **Yupei Jian:** Funding acquisition (equal); Investigation (equal); Project administration (equal); Writing – review & editing (equal). **Quanke Su:** Investigation (equal); Project administration (equal); Resources (equal); Writing – review & editing (equal). **Guobiao Hu:** Conceptualization (lead); Formal analysis (equal); Funding acquisition (equal); Investigation (equal); Methodology (equal); Project administration (equal); Resources (equal); Supervision (equal); Writing – review & editing (lead).

DATA AVAILABILITY

The data that support the findings of this study are available from the corresponding authors upon reasonable request.

REFERENCES

[1]S. Rezaei, A. Rahimi, J. Parvizian, S. Mansoorzadeh, and A. Düster, "A rectified unidirectional rotary PTO for two-body wave energy converters," Ocean Eng. **279**, 114507 (2023).
[2]R. Liu, C. Pan, H. Zhou, H. Xia, and L. He, "Enhancement ultra-low-frequency wave energy harvesting through a piezoelectric energy harvester based on C-shaped cantilever beams," Renewable Energy **256**, 124220 (2026).
[3]Y. Wang, H. Du, H. Yang, Z. Xi, C. Zhao, Z. Qian, X. Chuai, X. Peng, H. Yu, Y. Zhang, X. Li, G. Hu, H. Wang, and M. Xu, "A rolling-mode triboelectric nanogenerator with multi-tunnel grating electrodes and opposite-charge-enhancement for wave energy harvesting," Nat. Commun. **15**(1), 6834 (2024).
[4]X. Li, C.-A. Chen, S. Chen, Q. Xiong, J. Huang, S. Lambert, J. Keller, R. G. Parker, and L. Zuo, "Dynamic characterization and performance evaluation of a 10-kW power take-off with mechanical motion rectifier for wave energy conversion," Ocean Eng. **250**, 110983 (2022).
[5]R. Ahamed, K. McKee, and I. Howard, "Advancements of wave energy converters based on power take off (PTO) systems: A review," Ocean Eng. **204**, 107248 (2020).
[6]W. Liu, Y. Li, H. Tang, Z. Zhang, X. Wu, J. Zhao, L. Zeng, M. Tang, and D. Hao, "The nexus of sustainable fisheries: A hybrid self-powered and self-sensing wave energy harvester," Ocean Eng. **295**, 116996 (2024).
[7]R. Liu, H. Wang, L. Sun, X. Li, and L. He, "A lever-type piezoelectric wave energy harvester based on magnetic coupling and inertial vibration," Sustainable Energy Technol. Assess. **62**, 103605 (2024).
[8]L. Lu, H. Sun, L. Han, Z. Zhang, H. Cao, W. Wang, X. Wu, and X. Lyu, "Omnidirectional hybrid wave energy harvester for self-powered sensors in sea-crossing bridges," Ocean Eng. **287**, 115829 (2023).
[9]L. Qi, H. Li, X. Wu, Z. Zhang, W. Duan, and M. Yi, "A hybrid piezoelectric-electromagnetic wave energy harvester based on capsule structure for self-powered applications in sea-crossing bridges," Renewable Energy **178**, 1223–1235 (2021).
[10]J. Liu, X. Li, L. Yang, X. Wu, J. Huang, J. Mi, and L. Zuo, "Achieving optimum power extraction of wave energy converters through tunable mechanical components," Energy **291**, 130322 (2024).
[11]H. Qiu, H. Wang, L. Xu, M. Zheng, and Z. L. Wang, "Brownian motor inspired monodirectional continuous spinning triboelectric nanogenerators for extracting energy from irregular gentle water waves," Energy Environ. Sci. **16**(2), 473–483 (2023).
[12]W. Chen, Y. Lu, Z. Liu, S. Zhou, R. Law, E. Q. Wu, and L. Zhu, "Design, dynamic modeling, and modal analysis of an in-situ umbrella-shaped wave energy converter through experiment validation," IEEE/ASME Trans. Mechatron. **30**, 5879 (2025).
[13]X. Dai, N. Wu, Y. He, X. Zeng, Y. Liang, and C. Xu, "A bistable wave energy harvester with orientation adaptive characteristics actuated by a rotating driving magnet," Renewable Energy **251**, 123487 (2025).
[14]T. Tang, Y. Li, M. Huang, M. Mei, Z. Wang, F. Zha, L. Sun, and H. Liu, "Ultra-low-frequency and high-power Mag-Boost mechanism for ocean wave energy harvesting," Environ. Prog. Sustainable Energy **213**, 115463 (2025).
[15]Q. Cai and S. Zhu, "Applying double-mass pendulum oscillator with tunable ultra-low frequency in wave energy converters," Appl. Energy **298**, 117228 (2021).
[16]X. Zeng, N. Wu, J. Fu, Y. He, and X. Dai, "Design, modeling and experiments of bistable wave energy harvester with directional self-adaptive characteristics," Energy **311**, 133454 (2024).
[17]R. Liu, L. He, B. Yang, X. Li, L. Zhang, and F. Zhong, "A low-frequency piezoelectric wave energy harvester based on segmental beam and double magnetic excitation," Energy **302**, 131790 (2024).

[18]C. Xiong, N. Wu, J. Fu, C.-T. Ng, J. Wu, Y. He, and X. Zeng, "Wave-inspired piezoelectric bistable energy harvester considering stress distribution: Design, simulation and experimental investigation," Eng. Struct. **316**, 118535 (2024).
[19]Y. Liu, P. Wang, W. Ma, W. Jiang, S. Yao, and D. Zhang, "Fish- and fish-school-inspired ocean current energy harvester array with triboelectric nanogenerator," Device **3**, 100943 (2025).
[20]C. Zhang, L. He, L. Zhou, O. Yang, W. Yuan, X. Wei, Y. Liu, L. Lu, J. Wang, and Z. L. Wang, "Active resonance triboelectric nanogenerator for harvesting omnidirectional water-wave energy," Joule **5**(6), 1613–1623 (2021).
[21]J. Graves, Y. Kuang, and M. Zhu, "Scalable pendulum energy harvester for unmanned surface vehicles," Sens. Actuators, A **315**, 112356 (2020).
[22]H. Lou, T. Wang, and S. Zhu, "Design, modeling and experiments of a novel biaxial-pendulum vibration energy harvester," Energy **254**, 124431 (2022).
[23]R. Liu, L. He, X. Liu, S. Wang, L. Zhang, and G. Cheng, "A review of collecting ocean wave energy based on piezoelectric energy harvester," Sustainable Energy Technol. Assess. **59**, 103417 (2023).
[24]Y. Wang, X. Liu, Y. Wang, H. Wang, H. Wang, S. L. Zhang, T. Zhao, M. Xu, and Z. L. Wang, "Flexible seaweed-like triboelectric nanogenerator as a wave energy harvester powering marine internet of things," ACS Nano **15**(10), 15700–15709 (2021).
[25]Y. Li, Y. Li, Y. Wang, M. Xiao, H. Tang, Y. Zi, J. Wang, X. Li, W.-H. Liao, and G. Hu, "From nature's deadly strike to safety protection: Mantis shrimp-inspired ultrafast energy transformation for smart surveillance," Device **4**, 100903 (2026).
[26]Y. Li, X. Peng, Y. Li, D. Li, and G. Hu, "Catapult mechanism-enabled push-button energy harvester designed for capturing ultra-low frequency motion," Mech. Syst. Signal Process. **225**, 112268 (2025).
[27]B. Zhao, Y. Wang, S. Huang, T. Tian, X. Liao, W. Wang, and Z. Li, "High-durability pendulum-structured TENG-EMG hybrid with stacked liquid-solid triboelectric layers for efficient low-frequency ocean wave energy capture," Chem. Eng. J. **523**, 168505 (2025).
[28]T. Zhao, Z. Li, B. Niu, G. Xie, L. Shangguan, M. Zhang, Y. Zhu, Y. Ma, C. Hu, and Y. Li, "A pendulum-based nanogenerator for high-entropy wave energy harvesting," Nat. Commun. **16**(1), 5480 (2025).
[29]B. Yang, L. He, Z. Liu, L. Feng, L. Zhang, and W. Fan, "An oscillating float-type piezoelectric-triboelectric-electromagnetic hybrid wave energy harvester used in fish-attracting lamp," Smart Mater. Struct. **33**(9), 095021 (2024).
[30]L. He, R. Liu, X. Liu, X. Zheng, L. Zhang, and J. Lin, "A piezoelectric-electromagnetic hybrid energy harvester for low-frequency wave motion and self-sensing wave environment monitoring," Energy Convers. Manage. **300**, 117920 (2024).
[31]M. Cai and W.-H. Liao, "Toward high-performance wrist-worn energy harvester via hybrid approach," IEEE/ASME Trans. Mechatron. **30**(1), 469–481 (2025).
[32]M. Cai and W.-H. Liao, "High-power density inertial energy harvester without additional proof mass for wearables," IEEE Internet Things J. **8**(1), 297–308 (2021).
[33]X. Hou, L. Niu, S. Qian, D. Hu, J. Hou, S. Shi, W. Geng, J. He, and X. Chou, "Electromagnetic energy harvester based on bidirectional vibration to unidirectional rotation conversion for environmental low-frequency vibration energy harvesting," IEEE Trans. Power Electron. **39**(2), 1932–1941 (2024).
[34]L. Zhao, H. Zou, X. Xie, D. Guo, Q. Gao, Z. Wu, G. Yan, K. Wei, and W. Zhang, "Mechanical intelligent wave energy harvesting and self-powered marine environment monitoring," Nano Energy **108**, 108222 (2023).
[35]S. Jia, C. Zeng, G. Shi, J. Xu, Y. Xia, W. Zeng, X. Wang, and H. Xia, "A hybrid wave vibration energy harvester with electromagnetic double-speed and piezoelectric up-frequency driven by a rotating ball," Smart Mater. Struct. **33**(6), 065023 (2024).
[36]T. Wang and H. Wang, "Multistable pendulum wave energy harvesting under multidirectional irregular excitations," IEEE/ASME Trans. Mechatron. **29**(4), 3175–3183 (2024).